

Neutron Spin Echo Optics

Norio Achiwa, Masahiro Hino, *Seiji Tasaki, *Toru Ebisawa, *Tsunekazu Akiyoshi
 and *Takeshi Kawai

Department of Physics, Faculty of Science, Kyushu University, Fukuoka 812, JAPAN
Research Reactor Institute, Kyoto University, Kumatori, Osaka 590-04, JAPAN

(Received 18 March 1996; accepted 19 July 1996)

Recently proposed experiments for neutron spin optics were extensively carried out using a transverse neutron spin echo (NSE) instrument for the neutron optics, which was installed at CN3 guide tube of the cold neutron source at Kyoto University Reactor(KUR). By setting a crystal or a magnetic film in one of the Larmor precession fields, a phase shift and a change of the NSE signals through the sample were observed. The shift of NSE signal through the sample was interpreted as the phase change between \uparrow and \downarrow spin wave functions of neutron as in the following cases: (1) measurement of refractive index of Si crystal by forward scattering NSE method, (2) measurement of traversal times through a magnetic thin film (Fe, or permalloy) above the critical angle of total reflection by the Larmor clock,(3) neutron spin interference of tunneling neutrons through the magnetic thin films and (4) phase interference of neutron spin wave functions in the forward scattering through a magnetic multilayer in case of the Bragg reflection observed by NSE signals.

KEYWORDS: Larmor precession, neutron spin echo, neutron optics, polarized neutron

§.1. Introduction

Importance of the neutron Larmor precession to the field of neutron optics was first realized through the verification of 4π periodicity of spinor wave function by Rauch *et al.*¹⁾ and Werner *et al.*²⁾ by means of polarized neutron interferometry. The coherent properties of a neutron in the process of Larmor precession was also discussed by Mezei.^{3,4)} For a spin $\frac{1}{2}$ neutron, a stationary spin wave function rotating in space in the perpendicular plane to a magnetic field H is expressed by a coherent superposition of the two spin states as follows,

$$|\psi(\mathbf{r}, t=0)\rangle = \frac{1}{\sqrt{2}} \left[e^{ik_+r} \begin{pmatrix} 1 \\ 0 \end{pmatrix} + e^{ik_-r} \begin{pmatrix} 0 \\ 1 \end{pmatrix} \right], \quad (1.1)$$

where $\begin{pmatrix} 1 \\ 0 \end{pmatrix}$ and $\begin{pmatrix} 0 \\ 1 \end{pmatrix}$ are the eigenstates of \uparrow and \downarrow spin wave function. Here, the effect of the magnetic field appears in the wave numbers k_{\pm} and in the refractive indices n_{\pm} :

$$k_{\pm} = k_0 n_{\pm} = k_0 \left(1 \mp \frac{\mu H}{E} \right)^{1/2}, \quad (1.2)$$

where $E = \hbar^2 k_0^2 / 2m$ and m , μ , H and k_0 are the mass, the magnetic moment of neutron, the applied magnetic field, and the wave number in the absence of field, respectively. We will look at the phase difference between \uparrow and \downarrow spin wave functions:

$$\Delta\phi = (\mathbf{k}_+ - \mathbf{k}_-) \mathbf{r} = \delta \mathbf{k} \mathbf{r} \quad (1.3)$$

$$= k_0 (n_+ - n_-) \mathbf{r} \quad (1.4)$$

$$\approx -k_0 \frac{\mu H}{E} \mathbf{r}, \quad (1.5)$$

for $\mu H \ll E$. This relation is rewritten by using the Larmor frequency $\omega_L = 2\mu H/\hbar$ as follows:

$$\Delta\phi = -\frac{\omega_L}{v} \mathbf{r}, \quad (1.6)$$

where v is the neutron velocity. Here, the Larmor frequency is directly proportional to the phase difference between \uparrow and \downarrow spin wave function. If we have extra phase delays $\delta\eta_{\pm}$ in both of the spin wave functions, respectively, by inserting a phase shifter in the magnetic field, then

$$|\psi(\mathbf{r}, t=0)\rangle = \frac{1}{\sqrt{2}} \left[e^{i\delta\eta_+} e^{ik_+r} \begin{pmatrix} 1 \\ 0 \end{pmatrix} + e^{i\delta\eta_-} e^{ik_-r} \begin{pmatrix} 0 \\ 1 \end{pmatrix} \right], \quad (1.7)$$

and the expectation values of $\langle S_x \rangle$, $\langle S_y \rangle$ and $\langle S_z \rangle$ are given by

$$\langle S_x \rangle = \hbar \langle \psi | \frac{1}{2} \sigma_x | \psi \rangle = \hbar \cos(\Delta\phi + \delta\eta_+ - \delta\eta_-), \quad (1.8)$$

$$\langle S_y \rangle = \hbar \langle \psi | \frac{1}{2} \sigma_y | \psi \rangle = -\hbar \sin(\Delta\phi + \delta\eta_+ - \delta\eta_-), \quad (1.9)$$

$$\langle S_z \rangle = \hbar \langle \psi | \frac{1}{2} \sigma_z | \psi \rangle = 0, \quad (1.10)$$

where σ_x , σ_y and σ_z are the Pauli matrices defined by

$$\sigma_x = \begin{pmatrix} 0 & 1 \\ 1 & 0 \end{pmatrix}, \quad \sigma_y = \begin{pmatrix} 0 & -i \\ i & 0 \end{pmatrix}, \quad (1.11)$$

$$\sigma_z = \begin{pmatrix} 1 & 0 \\ 0 & -1 \end{pmatrix}$$

Then, we will get an extra spin rotation of $\delta\eta = \delta\eta_+ - \delta\eta_-$ by inserting the phase shifter.

This principle opens many applications of Larmor precession for forward scattering of neutrons through magnetic materials. Büttiker⁵⁾ extended the principle to a more general case; the phase shift due to a tunneling potential was also interpreted as the Larmor precession. Baryshevskii *et al.*⁶⁾ and Frank⁷⁾ discussed an additional precession of the neutron spin through nonmagnetic matter in an applied field. Baryshevskii proposed neutron spin interferometry using a neutron spin echo (NSE) spectrometer. The NSE method developed by Mezei⁸⁾ is one of the best principles to measure Larmor precession. The NSE method utilized the phase convergence of Larmor precession by a π spin flipper after passing one of the two precession magnetic fields, which allows one to measure the shift of Larmor precession very precisely. The small changes of neutron velocity by inelastic neutron scattering processes are usually measured by the NSE method. New applications of NSE are possible if we insert a sample in one of the Larmor precession fields and measure the additional spin rotation.

We will extensively apply the new NSE method for several interesting optical phenomena by using a transverse neutron spin echo spectrometer⁹⁾ installed on the CN-3 guide tube¹⁰⁾ of the cold neutron source at Kyoto University Reactor (KUR).

- i. Measurement of the refractive index of Si crystals by forward scattering NSE method.
- ii. Multiple elastic forward scattering through Be polycrystals observed by NSE method.
- iii. Measurement of traversal times through magnetic thin films (Fe, permalloy) above the critical angle of total reflection by the Larmor clock.
- iv. Neutron spin interference of tunneling neutrons through magnetic thin films.
- v. Phase interference of neutron spin wave functions in case of Bragg reflection observed by NSE signals.

§.2. Measurement of the refractive index by Larmor precession¹¹⁾

We will insert a piece of silicon single crystal in one of the precession fields of the transverse NSE spectrometer and observe an additional Larmor precession as shown in Fig.1(b).

The condition for spin echo is given as

$$\delta N = N_0 - N_1 = \frac{\gamma_L}{2\pi} \left[\frac{H_0 l_0}{v_0} - \frac{H_1 l_1}{v_1} \right] = 0, \quad (2.1)$$

where $\gamma_L = 2.916$ kHz/Oe, N is the number of Larmor precessions, l the length of the magnetic field H , v the neutron velocity, and the subscripts 0 and 1 mean the situation before and after the scattering, respectively.

A refractive index of neutrons, n , passing through a nonmagnetic material is derived from the optical potential $U = (2\pi\hbar^2/m)N_p b$, where N_p is the nuclear density, and b , the coherent scattering length. While in a magnetic material,

$$n_{\pm}(U) = \left(1 - \frac{U}{E} \mp \frac{\mu B}{E} \right)^{1/2} \quad (2.2)$$

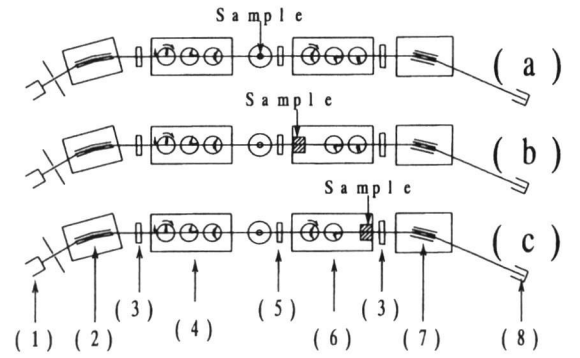


Fig. 1. The design of the new NSE method using the transverse NSE instrument. The sample was set at normal NSE position (a), at the entrance (b) and at the exit (c) of second Larmor precession field. The elements of the NSE instrument: (1)CN-3 supermirror neutron guide tube, (2)Soller type Double reflection supermirror polarizer¹²⁾, (3) $\pi/2$ spin flipper coil, (4)First Larmor precession field, (5) π spin flipper coil, (6)Second Larmor precession field, (7)Soller type supermirror analyzer, (8) ^3He neutron detector.

where B is the magnetic induction. Since the neutron velocity changes in the sample only for pure forward scattering, the refractive index is related to the shift of the echo point against the sample length D (see Baryshevskii⁶⁾ *et al.*).

The phase shift of the Larmor precession just after passage of the matter is given by the formula

$$\begin{aligned} \varphi &= k_0 [n_+(U) - n_-(U)] D \quad (2.3) \\ &\approx -k_0 \frac{\mu B}{E} D - k_0 \frac{\mu B}{E} \frac{U}{2E} D = \varphi_0 + \Delta\varphi \quad (2.4) \end{aligned}$$

$$\varphi_0 = -\omega_L \frac{D}{v_0}, \quad \text{and} \quad \Delta\varphi = -\omega_L \frac{D}{v_0} (1-n), \quad (2.5)$$

where, $k_0 = \sqrt{2mE}/\hbar$, $v_0 = \hbar k_0/m$, $\omega_L = 2\mu B/\hbar$ and the approximations $\mu B/E \ll 1$ and $U/E \ll 1$ are used in getting $\Delta\varphi$ and φ_0 .

The measurement of the refractive index at $q \approx 0$ needs to eliminate the non-optical factors, such as inelastic and multiple elastic neutron forward scattering. The NSE signal might be affected by the following four physical phenomena: (i)refractive index of neutron in a sample, (ii) magnetic susceptibility of a sample, (iii)multiple elastic scattering process and (iv) inelastic forward scattering. Setting a sample at the normal position (Fig.1(a)), the NSE signal is affected by (ii) and (iv). At the entrance (Fig.1(b)) of the second Larmor precession field, the NSE signal is affected by (i)~(iv). At the exit (Fig.1(c)), the NSE signal is affected by (i)~(iii).

The difference of polarizations of the NSE signals measured at two sample positions at the entrance and the exit gives inelastic neutron forward scattering processes. The multiple elastic scattering process changes the path length of neutrons through the sample. Comparing the NSE signals, therefore, measured at normal sample position and at the entrance of the second Larmor precession field, the multiple elastic process is estimated by

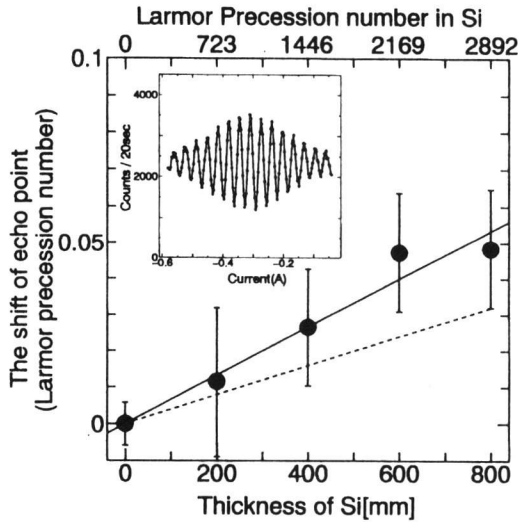


Fig. 2. The shift of NSE signals of 3000 turns measured by changing neutron path length of Si single crystal. The NSE signal without Si is inserted. The straight solid and dotted lines correspond to the observed and theoretical refractive index of neutron, respectively.

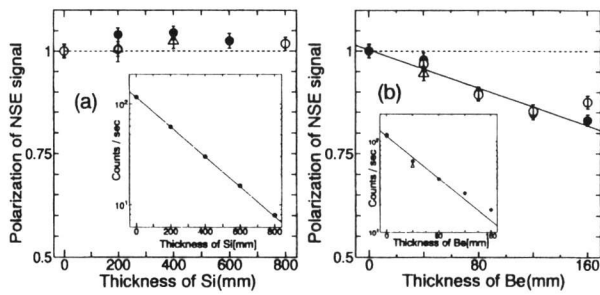


Fig. 3. Polarization of the NSE signals versus thickness of sample of neutron through, (a) Si single crystal of 200, 400, 600 or 800mm long, (b) Be polycrystal of 40, 80, 120 or 160mm long, for the total Larmor precessions of 2010 turns. The polarization was normalized by the polarization of NSE signal without a sample. Transmittance of direct neutrons through sample is inserted to each figures. The closed circle (●), open circle (○) and open triangle (△) indicate the polarizations measured at the exit and at the entrance of the second Larmor precession field and at sample position of normal NSE method, respectively.

the polarization dependence of the NSE signals with sample length. The shift of the echo point was measured by changing the neutron path length of a Si single crystal as shown in Fig.2. The NSE signal without Si is inserted in Fig.2.

The dotted line indicates the theoretical line for the shift by neutron refractive index of the Si single crystal in the second Larmor precession field. This is the first experimental evidence of neutron refractive index determined by NSE method. The experimentally determined neutron refractive index of Si is $1 - (1.85 \pm 1.16) \times 10^{-5}$ for 5.7\AA . The deviation of refractive index from 1 is 1.7 times larger than the theoretical value.

The variation of the polarization of the NSE signal was measured by changing the neutron path length of Si single

crystal and Be polycrystal, which are shown in Fig.3(a) and 3(b), respectively.

The closed circle, open circle and open triangle indicate polarization of the NSE signal measured at the exit and at the entrance of the second Larmor precession field and at the normal sample position, respectively. Though neutron transmittances through the Si crystal of 800mm long were 6.7%, the variation of polarization of the NSE signals was not detected. This is the proof that the elastic multiple scattering and the inelastic processes are not important for determination of refractive index for the Si crystal. On the other hand, the clear dependence in polarization of the NSE signal from the sample length was measured for Be polycrystals, which is due to multiple scattering by grain boundaries. The multiple forward scattering in the Be polycrystal contains various distributions of neutron path length. Then, the amplitude of the NSE signal, $P(L)$ with L the sample length, is the average of echo function with respect to the neutron path length l_i ,

$$P(L) = \langle \cos \phi_i(L) \rangle. \quad (2.6)$$

The polarization dependence of sample length seems to be linear as shown in Fig.3(b). The contribution from inelastic neutron forward scattering was obscured by experimental error in case of Be polycrystals.

§.3. Larmor precession through a magnetic thin film¹³⁾

Let us consider Larmor precession through a magnetic thin film when the incident angle approaches to the critical angle of total reflection with decreasing angle. Usually this problem is reduced to that of a one dimensional Schrödinger equation perpendicular to the film plane with a magnetic and a nuclear square potential barrier in the film. Büttiker has shown that additional Larmor precession through a magnetic film is proportional to the phase difference of neutron wave functions between those of \uparrow and \downarrow spin.

The wave function of the incident beam in Larmor precessing in an external field is given by

$$|\psi\rangle = \frac{1}{\sqrt{2}} \begin{pmatrix} e^{i\delta_+} \\ e^{i\delta_-} \end{pmatrix} e^{ik_{\perp}r} \quad (3.1)$$

where the $\delta = \delta_+ - \delta_-$ is the incident Larmor phase and the extra phase is added after transmitting the magnetic film.

The additional precession $\Delta\phi = \Delta\phi_+ - \Delta\phi_-$ is given by the following definition of the phases,

$$\begin{aligned} \tan(\Delta\phi_+) &= \frac{k_+^2 + \kappa_+^2}{2k_+ \kappa_+} \tan(\kappa_+ d), \\ \tan(\Delta\phi_-) &= \frac{k_-^2 + \kappa_-^2}{2k_- \kappa_-} \tan(\kappa_- d). \end{aligned} \quad (3.2)$$

Here d is the thickness of the magnetic film; wave number in the precession field H is given by $k_{\pm} = \sqrt{2m(E \mp |\mu H|)} / \hbar$; $E = (\hbar k_{\perp})^2 / 2m$; and the wave number in the magnetic film is given by $\kappa_{\pm} = \sqrt{2m(E - (U \mp |\mu B|))} / \hbar$.

Now we will simulate the NSE phase shifts through the magnetic film measured at various incident angles above

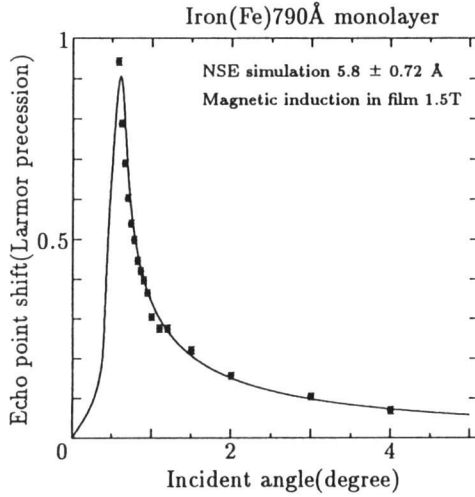


Fig. 4. The shift of NSE signals transmitted through a magnetic iron film with thickness of 790Å as a function of incident angle. The closed circles indicate the measured shift and the solid line indicates the calculated values from matrix analysis of neutron spin rotation and of one-dimensional square potential for Schrödinger equation. Here, the nuclear and the magnetic potentials are assumed to be 209neV and 90.4neV, respectively. The maximum traversal time at the critical angle is estimated to be 2.2×10^{-8} sec.

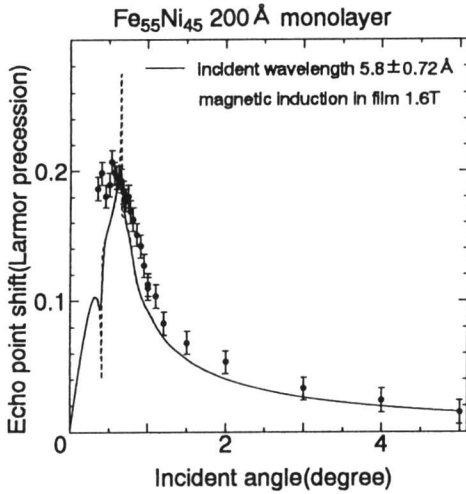


Fig. 5. The shift of NSE signals through magnetic permalloy45 thin film with thickness of 200Å as a function of incident angle. The closed circles indicate the measured phase shift and the solid line indicates calculated phase difference based on one-dimensional square potential for Schrödinger equation. The dotted vertical lines indicate the critical angles of total reflection for ↑ and ↓ neutrons with the wavelength 5.8Å. Here the nuclear potential U_{nuc} and the magnetic potential U_{mag} are assumed to be 220neV and 108.5neV, respectively.

the critical angle of both ↑ and ↓ spin neutrons.

After transmission through the magnetic film, ↑ and ↓ spin neutrons have different phases in the spatial wave function. Figure 4 shows the shifts of NSE signals (echo points) at various incident angles to an iron film with a thickness of 790Å.

Here using the nuclear and magnetic potentials of the iron film 209neV and 90.4neV, respectively, the observed

NSE shifts are well reproduced by the calculated precessions, $\Delta\phi = \Delta\phi_+ - \Delta\phi_-$ in Eq.(3.2).

The extra Larmor precession can be interpreted in terms of a Larmor time τ , by following Büttiker,

$$\omega_L \tau = \Delta\phi = \Delta\phi_+ - \Delta\phi_- . \quad (3.3)$$

This time τ is just the traversal time of the neutron spent inside the magnetic film. The maximum traversal time at the critical angle through an iron film with the thickness of 790Å is estimated to be 2.2×10^{-8} sec. For incident angles much larger than the critical angle of the total reflection, the Larmor precession can be approximated as,

$$\Delta\phi = \kappa_{\text{nuc}} d \frac{\mu B}{E} , \quad (3.4)$$

here d is the thickness of the magnetic layer, and $\kappa_{\text{nuc}} = \sqrt{2m(E - U)}/\hbar$

§.4. Larmor phase due to tunneling potential ¹⁴⁾

When Larmor precessing neutrons are incident on a magnetic thin film of iron or permalloy at a smaller glancing angle than the critical angle of total reflection for ↑ spin, the ↑ spin neutrons are totally reflected and the ↓ neutrons pass through. But if the magnetic film is thin enough to tunnel, the tunneling ↑ neutron can coherently couple with ↓ neutrons after passing through the magnetic film, resulting an extra Larmor precession. Again using the one-dimensional squared tunneling potential for the ↑ neutron, the extra Larmor precession is given by $\Delta\phi = \Delta\phi_+ - \Delta\phi_-$ which is calculated by the following equations, instead of Eq.(3.2),

$$\begin{aligned} \tan(\Delta\phi_+) &= \frac{k_+^2 - \kappa_+^2}{2k_+ \kappa_+} \tanh(\kappa_+ d) , \\ \tan(\Delta\phi_-) &= \frac{k_-^2 + \kappa_-^2}{2k_- \kappa_-} \tan(\kappa_- d) . \end{aligned} \quad (4.1)$$

Here the wave numbers are defined similarly as in Eq.(3.2) except $\kappa_+ = \sqrt{2m(U + |\mu B|) - E}/\hbar$ for $E < (U + |\mu B|)$.

Now we have measured a phase shift of NSE signals through permalloy45 (Fe₅₅Ni₄₅) film with thicknesses of 200Å across the critical angle as shown in Fig.5. Below the critical angle of ↑ neutron for permalloy45 (Fe₅₅Ni₄₅) film with thickness of 200Å, the NSE signal could be observed though the amplitude of the NSE signal decreases. The shift of the NSE signal through the permalloy film was maximized at the critical angle. The shift of NSE signal is well reproduced by the theoretical curves based on Eq.(4.1).

If the concept of Larmor precession is also effective in the tunneling state of neutrons, the tunneling time can be obtained using the Larmor time as discussed in Eq.(3.3). Using the magnetic induction of 1.8T in the permalloy film of 200Å, the tunneling time is estimated to be 3.6×10^{-9} sec.

Recent theoretical estimation of tunneling time using Nelson's stochastic approach by Ohba *et al.*¹⁵⁾ beautifully explains the tunneling behavior in Fig.5. As for the tunneling problem, there are still many discussions going on Ref. 16.

§.5. Larmor precession through a magnetic multilayer

Permalloy45 (Fe₅₅Ni₄₅)-Ge magnetic multilayer film has periodic potential of 316neV-93neV for \uparrow spin neutrons and 124neV-93neV (almost constant) potential for \downarrow spin neutrons. When neutrons (Larmor precession) pass through the magnetic multilayer at Bragg condition, it is expected that the amount of extra Larmor precession shows an anomaly at the angle of Bragg condition. Due to the multiple reflection among the periodic magnetic potential for the \uparrow spin neutron, a part of \uparrow spin neutrons is reflected at the surface of the multilayer and the other part of them are transmitted through the magnetic multilayer with an extra phase of the wave function. After transmitting the multilayer, the wave function of \uparrow spin couples with that of the \downarrow spin, resulting an extra Larmor precession. Again we need to deal only with wave vector k_{\perp} perpendicular to the surface plane of multilayer. By solving the one-dimensional Schrödinger equation for the periodic magnetic potential, the wave function in the j -th multilayer in the state of Larmor precession is given by

$$\psi_{j\pm}(r) = A_{j\pm} \cdot e^{ik_{j\pm}r} + B_{j\pm} \cdot e^{-ik_{j\pm}r} \quad (5.1)$$

If we represent $\psi_{j\pm}(r)$ by a vector $\begin{pmatrix} A_{j\pm} \\ B_{j\pm} \end{pmatrix}$, at the first

interface $\psi_{0\pm}(r_0) = \begin{pmatrix} 1 \\ r_{\pm} \end{pmatrix}$ and at the last interface $\psi_{j\pm}(r_j) = \begin{pmatrix} t_{\pm} \\ 0 \end{pmatrix}$, using the reflection and the transmission coefficients r_{\pm} and t_{\pm} . These are related by a transfer matrix M_{\pm} (17) as

$$\begin{pmatrix} 1 \\ r_{\pm} \end{pmatrix} = \begin{pmatrix} M_{11\pm} & M_{12\pm} \\ M_{21\pm} & M_{22\pm} \end{pmatrix} \begin{pmatrix} t_{\pm} \\ 0 \end{pmatrix} \quad (5.2)$$

Solving Eq.(5.2), one can obtain transmission coefficients as $t_{\pm} = \sqrt{T_{\pm}} e^{i\Delta\phi_{\pm}}$, where T_{\pm} are the transmission probabilities. Then we get the extra Larmor precession $\Delta\phi = \Delta\phi_{+} - \Delta\phi_{-}$ through a magnetic multilayer.

$$\langle S_x \rangle = \hbar \cos(\Delta\phi_{+} - \Delta\phi_{-}) \frac{\sqrt{T_{+}T_{-}}}{T_{+} + T_{-}} \quad (5.3)$$

$$\langle S_y \rangle = -\hbar \sin(\Delta\phi_{+} - \Delta\phi_{-}) \frac{\sqrt{T_{+}T_{-}}}{T_{+} + T_{-}} \quad (5.4)$$

$$\langle S_z \rangle = \frac{\hbar}{2} \frac{T_{+} - T_{-}}{T_{+} + T_{-}} \quad (5.5)$$

Then, the amplitude of the NSE signal, P can be expressed by the transmission probabilities T_{\pm} as

$$P = P_0 \frac{|\langle S_{x,y} \rangle|}{|\langle S_{x,y} \rangle| + \frac{1}{2} |\langle S_z \rangle|} \quad (5.6)$$

$$= P_0 \frac{4\sqrt{T_{+}T_{-}}}{4\sqrt{T_{+}T_{-}} + |T_{+} - T_{-}|} \quad (5.7)$$

where P_0 is the NSE signal in the absence of the magnetic layer.

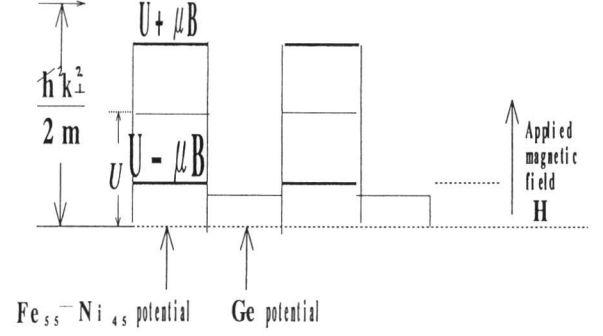


Fig. 6. One dimensional periodic potentials of permalloy45 (100Å) - Ge (50Å) multilayer of 17 bilayers for \uparrow and \downarrow neutron spins, respectively. The permalloy45-Ge magnetic multilayer film plays periodic potential of 316neV-93neV for \uparrow spin neutrons and 124neV-93neV almost constant potential for \downarrow spin neutrons.

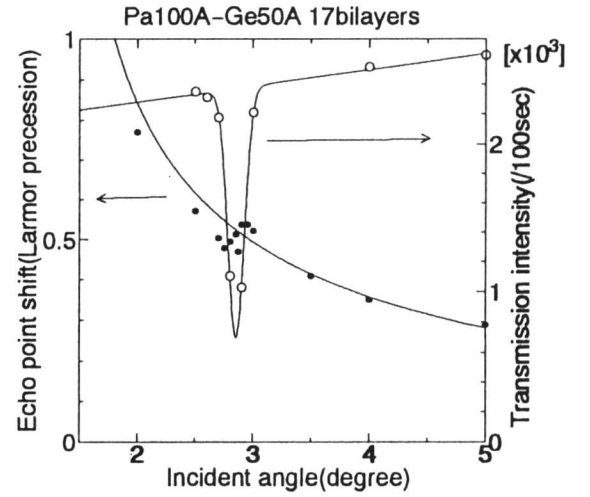


Fig. 7. The shift of NSE signals as well as transmission intensity through permalloy45 (100Å) - Ge(50Å) multilayer of 17 bilayers as a function of incident angle with the wavelength resolution of $\delta\lambda/\lambda = 0.03$ at $\lambda = 12.6\text{\AA}$. The closed circles represent the measured shift and the solid line indicates calculated phase differences based on the one-dimensional averaged square potential for the multilayer treated as a single layer. At the Bragg condition anomalous phase delay of the Larmor precession is seen.

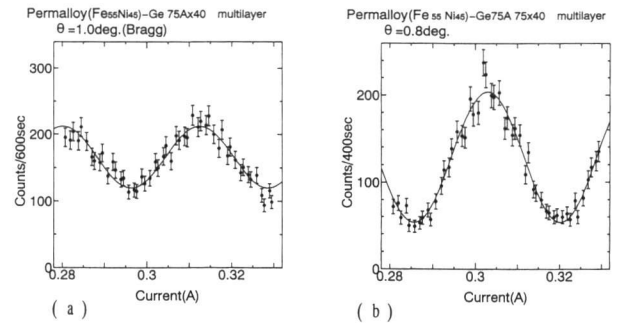


Fig. 8. The NSE signal of transmitted neutrons through permalloy45 - Ge multilayer of 20 bilayers each with thickness of 75Å; (a) at 1.0 deg = θ_{Bragg} and (b) at 0.8 deg. $< \theta_{\text{Bragg}}$ with the angular divergence of $\alpha = 1.0 \times 10^{-3}$ rad and with the wavelength resolution of $\delta\lambda/\lambda = 0.07$ at $\lambda = 5.8\text{\AA}$.

Figure 7 shows the shift of NSE signals across the Bragg angle where at the Bragg condition one can find the anomaly of the Larmor precession using the new spin and phase echo spectrometer installed at C3-1-2 cold neutron guide tube at JRR-3M.¹⁸⁾

Now we will look at the NSE signal at the Bragg condition through the permalloy45-Ge multilayer of 20 bilayers with each of thickness 75Å in Fig.8(a), comparing that with the off-Bragg condition as shown in Fig.8(b). The amplitudes of the NSE signal at the Bragg condition $\theta=1.0$ deg. and off Bragg position of $\theta=0.8$ deg. are expressed as the polarization $P=0.28$ and 0.60, respectively. This reduction of the polarization is caused by two reasons. At the Bragg condition only \uparrow neutrons are half reflected so the transmitted probabilities are $T_+=0.5$ and $T_-=1.0$. Then the other 50% of \uparrow neutrons pass through the multilayer with the Bragg condition and then couple with the transmitted \downarrow neutrons producing the Larmor precession as shown in Fig.8(a). This amplitude of NSE signal should be $P=0.85$ from Eq.(5.7). The observed ratio of $P_{ratio}=0.28/0.60$ is smaller than $P=0.85$. In order to explain the reduction of NSE amplitude there should be another reason. This is due to the effect of multiple scattering in a magnetic multilayer within the Bragg condition. If the multiple scattering process is all coherent, we must adopt Eq. (5.7). Then, the decrease of the NSE polarization should not occur. But if the angular divergence and wavelength resolution of the incident neutrons are not small enough, the usual transmitted NSE signal at the Bragg reflection reduces the polarization. When the multiple scattering processes are incoherent with each other, we should adopt then a equation similar to Eq. (2.6) as

$$P = \langle P_i \cos(\Delta\phi_{+i} - \Delta\phi_{-i}) \rangle. \quad (5.8)$$

The average should be done for every multiple reflection i . Then the further reduction of the polarization, $0.85 - \frac{0.28}{0.6} \approx 0.39$ can be explained.

§.6. Conclusion

Some new experimental results on neutron spin echo optics were first shown in the following cases:

- i. The refractive index of Si crystals was first determined by forward scattering NSE method as $1 - (1.85 \pm 1.16) \times 10^{-5}$ at 5.7Å.
- ii. Multiple elastic forward scattering through Be polycrystals was observed by NSE method through the linear path length dependence of the reduction of NSE amplitude.
- iii. By the measurement of traversal times through magnetic thin films (Fe, permalloy) above the critical angle of total reflection by the Larmor clock, the maximum traversal time through a magnetic iron film is estimated to be 2.2×10^{-8} sec.
- iv. Neutron spin interference of tunneling neutrons through the magnetic thin films was first observed. And the tunneling time is estimated to be $4 \pm 0.6 \times 10^{-9}$ sec for permalloy45 with thickness of 200Å.

- v. Phase delay of the Larmor precession in forward scattering through magnetic multilayers in case of the Bragg reflection observed by NSE signals.

The general principles in neutron spin echo optics was established as the forward scattering through a matter of magnetic or non-magnetic material in Larmor precession, bringing additional phase shift of the Larmor precession which is just the phase difference between the \uparrow and \downarrow spin wave function. The method has large intensity gain comparing the usual neutron interferometer, because we need no beam splitter and just look at the Larmor precession of the forward scattering through the sample.

After being transmitted through a single or a multilayer magnetic mirror, a spin echo amplitude can be expressed only by a function of transmission probabilities T_{\pm} as shown in Eq. (5.7). When the reflectivity is very high such as tunneling condition for \uparrow neutron or Bragg condition of \uparrow neutrons, the amplitude of the NSE signal is almost

proportional to the $\frac{4\sqrt{T_+}}{4\sqrt{T_+} + 1}$ when $T_- \sim 1$ and $T_+ \ll 1$. Thus

we have a large amount of intensity gain comparing a simple transmission measurement of T_+ . This is again due to the fact that a Larmor precession is a coherent superposition of \uparrow and \downarrow spin wave function.

The Larmor precession of a reflected case for a magnetic mirror would be also very interesting.

-
- 1) H. Rauch, A. Zeilinger, G. Badurek, A. Wilfling, W. Bauspiess and U. Bonse, *Phys. Lett. A* 54 (1975) 425.
 - 2) S.A. Werner, R. Colella, A.W. Overhauser and C.F.Eagan, *Phys. Rev. Lett.* 35 (1975) 1053.
 - 3) F. Mezei, in: *Imaging Processes and Coherence in Physics*, M.Schlenker et al., eds. *Lecture Notes in Physics* (Springer, Heidelberg, 1980) 282.
 - 4) F. Mezei, *Physica B* 151 (1988) 74-81.
 - 5) M. Büttiker, *Phys. Rev. B* 27 (1983) 6178.
 - 6) V.G. Baryshevskii, S.V. Cherepitsa and A.I. Frank, *Phys. Letters A* 153 (1991) 299.
 - 7) A.I. Frank, *Nucl. Inst. Method A* 284 (1989) 161.
 - 8) F. Mezei, ed., *Neutron Spin Echo, Lecture Notes in Physics* 128 (Springer, Heidelberg, 1980).
 - 9) N. Achiwa, M. Hino, S. Tasaki, T. Ebisawa and T. Akiyoshi, *JAERI-M93-228* (JAERI CONF2) (1993) 738.
 - 10) M. Hino, T. Akiyoshi, M. Sugiyama, N. Achiwa, Y. Eguchi, T. Ebisawa, S. Tasaki, T. Kawai, K. Yoneda and T. Kobayashi, *Annu. Rep. Res. Reactor Inst. Kyoto Univ.* 27 (1994) 196.
 - 11) M. Hino, N. Achiwa, S. Tasaki, T. Ebisawa and T. Akiyoshi, *Physica B* 213&214 (1995) 842.
 - 12) S. Tasaki, T. Ebisawa, N. Achiwa, T. Akiyoshi and S. Okamoto, *SPIE 983 Thin-Film Neutron Optical Devices* (1988) 144.
 - 13) M. Hino, N. Achiwa, S. Tasaki, T. Ebisawa, T. Akiyoshi and T. Kawai, in this proceedings.
 - 14) M. Hino, N. Achiwa, S. Tasaki, T. Ebisawa, T. Akiyoshi and T. Kawai, in this proceedings.
 - 15) I. Ohba, K. Imafuku and Y. Yamanaka, in this proceedings.
 - 16) see review article, R. Landauer, *Rev. Mod. Phys.* 66 (1994) 217.
 - 17) S. Yamada, T. Ebisawa, N. Achiwa, T. Akiyoshi and S. Okamoto, *Annu. Rep. Res. Reactor Inst. Kyoto Univ.* 11 (1978) 8.
 - 18) T. Ebisawa, S. Tasaki, Y. Otake and H. Funahashi, *Physica B* 213&214 (1995) 901.